Critical dynamics of cluster algorithms in the random-bond Ising model

Ulvi Kanbur[1] and Zeynep Demir Vatansever[2,*]
[1]*Department of Physics, Karabük University, Demir Çelik Campus, 78050 Karabük, Turkey*
[2]*Department of Physics, Dokuz Eylül University, TR-35160, Izmir-Turkey*

(Received 2 October 2023; accepted 2 February 2024; published 28 February 2024)

In the present work, we present an extensive Monte Carlo simulation study on the dynamical properties of the two-dimensional random-bond Ising model. The correlation time τ of the Swendsen-Wang and Wolff cluster algorithms is calculated at the critical point. The dynamic critical exponent z of both algorithms is also measured by using the numerical data for several lattice sizes up to $L = 512$. It is found for both algorithms that the autocorrelation time decreases considerably and the critical slowing-down effect reduces upon the introduction of bond disorder. Additionally, simulations with the Metropolis algorithm are performed, and the critical slowing-down effect is observed to be more pronounced in the presence of disorder, confirming the previous findings in the literature. Moreover, the existence of the non-self-averaging property of the model is demonstrated by calculating the scaled form of the standard deviation of autocorrelation times. Finally, the critical exponent ratio of the magnetic susceptibility is estimated by using the average cluster size of the Wolff algorithm.

DOI: 10.1103/PhysRevE.109.024140

I. INTRODUCTION

In statistical physics, Monte Carlo (MC) simulations are the main tools to study the phase transitions and critical phenomena [1–3]. The achievement of the maximum possible system size is of vital importance to reduce finite-size effects and obtain high-quality statistics. However, the critical slowing-down effect (the increase of the correlation time τ with system size near the critical point) limits the largest system size studied. As the critical point is approached, the correlation time of a finite system is expected to behave as $\tau \sim L^z$, where z is the dynamic exponent and L is the linear size of the system. Single-spin-flip dynamics, such as the Metropolis algorithm [4], considerably suffer from the critical slowing-down effect. For the two-dimensional Ising model, the local algorithms have a dynamic exponent around 2 [5] which requires long simulation times. Such drawbacks of local algorithms have led to the development of the cluster-flip dynamics as Swendsen-Wang (SW) [6] and Wolff [7] algorithms, which can produce small values of dynamic exponents and reduce the correlation times. The cluster algorithms are more efficient near the critical point than the local dynamics in the case of the pure Ising model ($z_{\text{local}} > z_{\text{cluster}}$) [2,8].

Magnetic systems in the presence of disorder, which is inevitable in realistic materials, have been explored intensively both theoretically and experimentally [9]. It has been revealed that quenched disorder can have significant effects on the critical and universal aspects of the systems. Quenched randomness is shown to soften the first-order phase transitions considerably [10]. On the other hand, the presence of random fields [11] and site dilution [12] may lead to distinct critical exponents than the pure models. The Harris criterion [13] states that if the specific heat exponent α_p of the pure system is positive ($\alpha_p > 0$), then the disorder is relevant and the system will have a new critical character, whereas if α_p is negative ($\alpha_p < 0$), the disorder will not affect the universality class of the system. Systems with zero specific heat exponent ($\alpha_p = 0$), such as the two-dimensional (2D) Ising model, are the marginal cases of the criterion and therefore the effects of site dilution [12,14–18], bond dilution [19–22], and bond randomness [23–27] on the statistical critical exponents of the Ising model have been of particular interest. The common view in recent studies is the strong universality hypothesis, which states that the disorder leads to a marginal irrelevance of randomness and the Ising universality class is preserved with additional logarithmic corrections. A significant number of works have been devoted to the 2D random-bond Ising model due to the exactly known critical temperature of the model as a function of disorder strength. For instance, critical properties of the Ising model [28–32] and Blume-Capel model [33–36] in the presence of bond randomness have been studied intensively. The general finding is the fact that the random-bond Ising model falls into the universality class of the ordinary Ising model through the logarithmic corrections in the specific heat.

An essential step toward understanding the critical phenomena in more sophisticated problems, for instance, in quantum spin models [37–39] and nonequilibrium phase transitions [40–43], is to study the disordered Ising model and its variants. The most widely used method for studying the critical properties of the Ising model is MC simulations. Since high-quality data is required for extracting the critical exponents, using the most suitable algorithm is necessary. Previous works indicate that the performance of an MC algorithm may change upon the inclusion of disorder effects. Accordingly, it becomes important to know the dynamic properties, such as autocorrelation times and the dynamic exponent of the algorithms near the critical point in the disordered spin models. On the other hand, despite the progress in the investigation

*Corresponding author: zeynep.demir@deu.edu.tr

of statistical critical exponents, the dynamic properties of the disordered Ising model and the effectiveness of the local and cluster algorithms are still under investigation. In an earlier study of the site-diluted simple cubic Ising model, the autocorrelation time and dynamic critical exponent of Swendsen-Wang and Wolff algorithms are shown to decrease when decreasing the concentration of magnetic sites [44]. Similarly, the cluster algorithms are found with lower values of dynamical critical exponents than the single-spin-flip Metropolis algorithm for the three-dimensional (3D) site-diluted Ising model with a dilution concentration $p = 0.85$ [45]. Moreover, the dynamics of cluster algorithms in a two-dimensional bond-diluted Ising model have been studied in a very recent study [22]. It has been reported that the Wolff algorithm suffers from longer correlation times in comparison with the pure Ising model and it has a dynamic exponent of $z_w \approx 1.75$, whereas the SW algorithm has shorter correlation times with a dynamic exponent of $z_{sw} = 0.09(4)$ [22].

To obtain a complete picture of the dynamic characteristics of MC cluster algorithms in disordered Ising models, in the present work we study the critical dynamics of the 2D random-bond Ising model by using Wolff and Swendsen-Wang cluster algorithms. By generating the disorder in the bonds from a bimodal distribution, we obtain the autocorrelation times and dynamic exponents at the critical point. Our detailed numerical analysis reveals that correlation times and critical exponents decrease with increasing the bond randomness in the system. Finally, we confirm that the introduction of the disorder increases the critical slowing-down effect in single-spin dynamics based on our simulation results on Metropolis algorithm.

The rest of the paper is organized as follows: In Sec. II we define the model and the observables we are interested in. We also describe the cluster algorithms applied in the present study. We present our numerical results in Sec. III. Our brief conclusions are given in Sec. IV.

II. MODEL AND SIMULATION DETAILS

In this work we study the bond-disordered square lattice Ising model with quenched, uncorrelated random exchange couplings. The model can be defined by the following Hamiltonian:

$$H = -\sum_{\langle ij \rangle} J_{ij} S_i S_j. \tag{1}$$

Here, the spin variables take the values of $S_i = \pm 1$ and summation runs over all nearest-neighbor pairs of spins. The ferromagnetic exchange interactions ($J_{ij} > 0$) are selected from a bimodal distribution of the type

$$\mathcal{P}(J_{ij}) = \tfrac{1}{2}[\delta(J_{ij} - J_1) + \delta(J_{ij} - J_2)]. \tag{2}$$

We fix the Boltzmann constant as $k_B = 1$ and the exchange interaction parameters as $J_1 + J_2 = 2$, with $J_1 > J_2$, and define the disorder strength as $r = J_2/J_1$ [27,39,41]. Throughout the work the disorder parameter is considered as the following: $r = 1$ (pure case), $r = 0.25/1.75$, and $r = 0.5/1.5$.

To examine the dynamics of the random-bond Ising model, we have used SW and Wolff cluster algorithms. The main idea underlying the Wolff algorithm is to build a cluster of spins and flip the spins in the cluster simultaneously. We apply the following procedure to complete one Wolff step:

(1) A seed spin from the lattice is chosen randomly.

(2) The neighboring spins of the seed spin, which are aligned in the same direction as the seed spin, are added to the cluster with a probability of $P_{\text{add}} = 1 - e^{-2J_{ij}/T}$.

(3) Each of the neighboring spins of the included spins in step 2 are examined and added with a probability P_{add} if they are aligned in the same direction. This step is repeated until there are no more spins taken into account to be included in the cluster.

In the case of the random-bond Ising model, the probability of inclusion of a neighboring spin in the cluster depends on the strength of the exchange interaction J_{ij} as different from the pure Ising model. The method for the construction of the clusters is equivalent to the above procedure in the SW algorithm. Conversely, instead of one cluster, the lattice is divided into N_c clusters and each of the clusters is flipped with a probability of 1/2. [1,2,6–8].

Our large-scale simulations include linear system sizes of $L = 16$, 24, 32, 48, 64, 96, 128, 192, 256, 384, 512 in the presence of periodic boundary conditions. For each disorder parameter mentioned above, we have performed simulations by using over 100 000 disorder realizations for sizes $L \leqslant 32$ and 10 000 disorder realizations for sizes $L \geqslant 48$. To measure the interested observables, the first 50 000 Monte Carlo sweeps (MCSs) are used after discarding 10 000 MCSs for thermal equilibration. Spin configurations are initialized in an ordered state in each random realization to obtain an efficient equilibration.

During the simulations we have measured the time-displaced autocorrelation function which is defined for an observable X at time t as

$$C_X(t) = \langle (X_i - \langle X \rangle)(X_{i+t} - \langle X \rangle) \rangle. \tag{3}$$

Here, $\langle \cdots \rangle$ denotes the thermal average. By using the autocorrelation function of the observable X, it is possible to determine the integrated autocorrelation time:

$$\tau_{X,\text{int}} = \frac{1}{2} + \sum_{t=1}^{\infty} \frac{C_X(t)}{C_X(0)}. \tag{4}$$

For large t the normalized autocorrelation function behaves exponentially [46]:

$$\frac{C_X(t)}{C_X(0)} \propto e^{-t/\tau_{X,\text{exp}}}, \tag{5}$$

from which one can extract the exponential autocorrelation time $\tau_{X,\text{exp}}$ for the quantity X. The numerical calculation of the integrated autocorrelation time suffers from systematic errors for large t values. We use the following approach for the estimation of the integrated autocorrelation time [46]. Firstly, the series in the Eq. (4) is terminated at a time t_{max} once the condition $t_{\text{max}} \geqslant 6\,\tau_{X,\text{int}}$ is met. Next, the trailing part of the series is completed by using the exponential autocorrelation time as in the following [47]:

$$\tau_{X,\text{int}}(t_{\text{max}}) = \tau_{X,\text{int}} - a\frac{e^{-t_{\text{max}}/\tau_{X,\text{exp}}}}{e^{1/\tau_{X,\text{exp}}} - 1}, \tag{6}$$

where a is the constant of the proportionality of Eq. (5). The main observable is the internal energy per site, $E = \langle H \rangle / N$, where N is the number of sites. The exponential and integrated correlation times are associated with the dynamical critical exponents z_{exp} and z_{int}, respectively, which govern the critical slowing down. We extract the dynamic critical exponents of the interested observable for both algorithms at each disorder parameter by using finite-size scaling of autocorrelation time.

In the SW algorithm, every spin gets a chance to be flipped in a single MCS, but in the Wolff case, only a portion (cluster) of spins have this possibility in a single MCS. The time between two algorithms is standardized by a factor $f = \langle C \rangle / N$, where $\langle C \rangle$ is the average cluster size in the Wolff algorithm. We calculate the quenched disordered average of the integrated autocorrelation time of the Wolff algorithm for the finite-size scaling analysis with the alternative procedure given in [48]. By using the convention $\tau_{X,\text{T}}$ (T = int, exp), we define the final averages of the autocorrelation times as $\tau_{X,\text{T}} = [f][\tau_{X,\text{T}}]$ for the Wolff algorithm. For every $\tau_{X,\text{T}}$ there is a corresponding dynamical critical exponent $z_{X,\text{T}}$ via the power law relation $\tau_{X,\text{T}} \sim L^{z_{X,\text{T}}}$ at the criticality.

To estimate the errors of the exponential and integrated autocorrelation times, we use the jackknife procedure after rebinning the data into 100 groups. Then the dynamical exponents are determined by a weighted least-squares data fit obtained from different system sizes.

III. RESULTS AND DISCUSSION

The 2D random-bond Ising model has the advantage that its exact phase diagram is available and exact critical temperature can be obtained from the relation [23]

$$\sinh(2J_1/T_C)\sinh(2rJ_1/T_C) = 1. \tag{7}$$

According to this relation, the critical temperatures of the interested disorder strengths in the present work are $T_C(r = 0.5/1.5) = 2.0781...$ and $T_C(r = 0.25/1.75) = 1.7781...$. Temperature dependence of specific heat curves is demonstrated in Fig. 1 for SW and Wolff algorithms at $r = 0.25/1.75$. The peak positions of the curves shift toward the exact critical temperature, shown by the vertical line, as the system size increases. Our pseudo-critical temperature values obtained from the peak position of the specific heat curves are compatible with the exact critical temperatures obtained via MC simulations results based on the Wang-Landau (WL) algorithm [27,30].

Next, we performed simulations at the critical temperature of the system to measure the autocorrelation times of SW and Wolff algorithms which are given in Table I. The common findings observed for both algorithms are as follows. Our results regarding the integrated and exponential autocorrelation times for the pure $2D$ Ising model ($r = 1$) are in excellent agreement with the previous findings in the literature for both algorithms [8,49]. Due to the introduction of a maximum cutoff in the sum of Eq. (4), one can see that $\tau_{E,\text{Exp}} > \tau_{E,\text{int}}$. Additionally, both integrated and exponential autocorrelation times take smaller values as the disorder strength is enhanced. Moreover, the autocorrelation times are substantially reduced in the robust disorder regime ($r = 0.25$). The effect of disorder on the dynamic properties of several disordered Ising

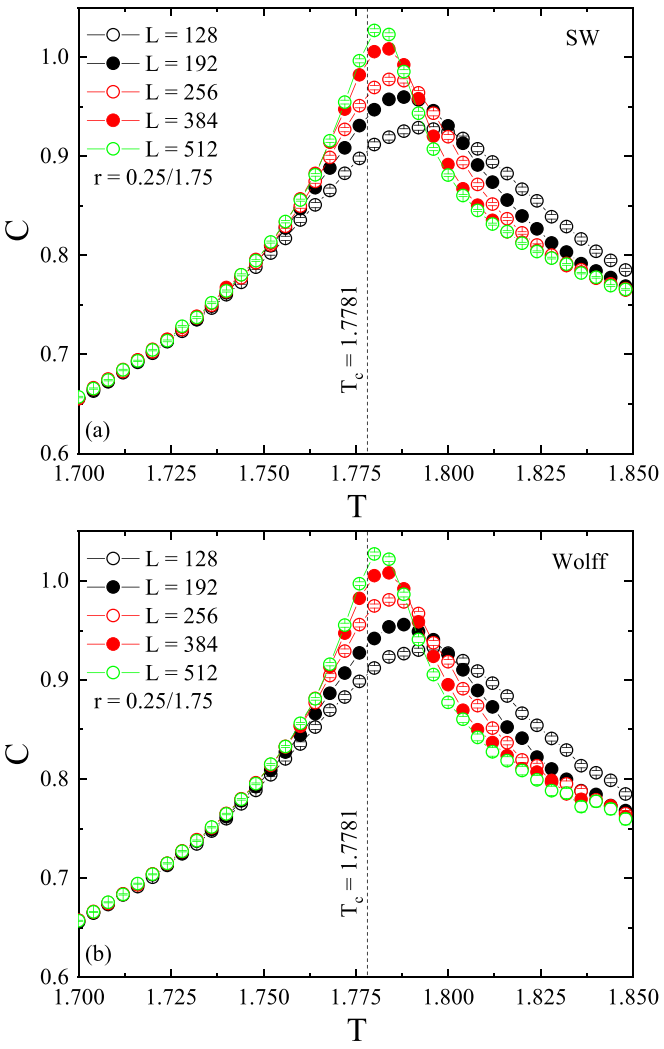

FIG. 1. Specific heat as a function of temperature at a disorder ratio of $r = 0.25/1.75$ obtained using (a) SW algorithm and (b) Wolff algorithm for several lattice sizes. The vertical dashed line indicates the exact critical temperature of the system. The system size increases from bottom to top in both figures.

systems has been explored in earlier studies [44,45,50]. The general finding is a reduction in autocorrelation times of cluster algorithms when introducing disorder in the model. Our numerical data are in agreement with these results.

Having obtained the correlation times, dynamic critical exponents of SW and Wolff algorithms are estimated. Figure 2 shows the integrated and exponential autocorrelation times as a function of lattice size with straight lines obtained by applying fits of the form $\tau \sim L^z$ for each disorder parameter considered. Calculated dynamic critical exponents are also given in Table II. The pure system ($r = 1$) has critical exponents at around $z \approx 0.25$ for both algorithms, in agreement with the literature [2]. Our numerical data also indicates that the disorder causes a decrement in the dynamic exponent of both algorithms. According to previous studies, cluster algorithms have lower critical exponents in comparison with the pure case for a 3D site-diluted Ising model [44,45]. Kole *et al.* have indicated that the Wolff algorithm suffers from the critical slowing-down effect when applied to the 2D bond-

TABLE I. Exponential and integrated correlation times obtained by SW and Wolff algorithm for different lattice sizes and disorder strengths.

		$\tau_{E,\text{exp}}$	$\tau_{E,\text{int}}$	$\tau_{E,\text{exp}}$	$\tau_{E,\text{int}}$
L	r	SW		Wolff	
16	1	3.2917(1)	3.245(1)	1.6829(1)	1.4304(5)
	0.5	2.8542(2)	2.766(2)	1.4349(1)	1.2145(6)
	0.25	2.3465(4)	2.209(1)	1.2681(2)	0.9998(9)
24	1	3.7673(2)	3.686(1)	1.9589(2)	1.6456(6)
	0.5	3.1917(2)	3.063(1)	1.6288(1)	1.3661(6)
	0.25	2.5655(1)	2.378(1)	1.4099(3)	1.103(1)
32	1	4.1162(4)	4.018(1)	2.1408(1)	1.8029(7)
	0.5	3.4312(1)	3.284(1)	1.7674(1)	1.4785(7)
	0.25	2.7322(1)	2.498(1)	1.5148(3)	1.180(1)
48	1	4.6781(6)	4.515(2)	2.4326(2)	2.0369(9)
	0.5	3.8098(1)	3.611(1)	1.9736(2)	1.6389(8)
	0.25	2.6826(2)	2.683(1)	1.6653(5)	1.288(1)
64	1	5.0017(2)	4.882(2)	2.6389(3)	2.209(1)
	0.5	4.1245(2)	3.853(1)	1.7644(4)	1.756(1)
	0.25	2.9929(2)	2.812(1)	2.1123(2)	1.366(1)
96	1	5.6780(3)	5.438(2)	2.9328(3)	2.463(1)
	0.5	4.5189(1)	4.202(2)	2.3311(2)	1.925(2)
	0.25	3.1838(6)	3.013(1)	1.9233(6)	1.477(1)
128	1	6.1354(7)	5.858(4)	3.1558(3)	2.651(2)
	0.5	4.8618(3)	4.458(2)	2.4846(3)	2.048(1)
	0.25	3.70197(4)	3.150(1)	2.0363(7)	1.558(1)
192	1	6.7529(1)	6.462(3)	3.4726(3)	2.926(2)
	0.5	5.3078(1)	4.838(2)	2.7043(3)	2.225(2)
	0.25	4.0235(5)	3.357(1)	2.1814(8)	1.672(2)
256	1	7.3389(1)	6.926(3)	3.7284(4)	3.130(2)
	0.5	5.6335(1)	5.110(2)	2.8664(5)	2.350(2)
	0.25	4.2559(5)	3.560(1)	2.2906(8)	1.752(2)
384	1	8.0734(1)	7.599(4)	4.080(4)	3.429(2)
	0.5	6.1617(3)	5.508(2)	3.0667(4)	2.531(2)
	0.25	4.6112(8)	3.724(1)	2.461(1)	1.870(2)
512	1	8.5760(2)	8.095(4)	4.310(4)	3.638(3)
	0.5	6.5031(1)	5.794(3)	3.2169(3)	2.666(2)
	0.25	4.8764(1)	3.886(1)	2.572(2)	1.952(2)

diluted Ising model because of the presence of isolated spins which are rarely visited during the simulations [22]. The same situation is not the case in our study, showing that using the Wolff algorithm weakens the critical slowing-down effect. This may be due to the absence of isolated spins and the presence of strengthened bonds in addition to weakened bonds in the random-bond model.

Our numerical data on the dynamic behavior of the random-bond Ising model also shows that the dynamic exponents of the SW and Wolff algorithms are very close to each other [49,51]. However, the autocorrelation times of the algorithms differ considerably, as shown in Table I. The Wolff algorithm has smaller autocorrelation times than the SW algorithm. This is related to the flip of every cluster generated in the Wolff algorithm as distinct from the SW algorithm, where half of the clusters generated are flipped at every MC step.

TABLE II. Dynamic critical exponents of SW and Wolff algorithms obtained from integrated and exponential autocorrelation times for energy for several disorder strengths.

	SW		Wolff	
r	z_{int}	z_{exp}	z_{int}	z_{exp}
1	0.254(4)	0.259(2)	0.250(5)	0.257(6)
0.5/1.5	0.200(3)	0.214(2)	0.207(4)	0.207(6)
0.25/1.75	0.156(1)	0.182(2)	0.175(4)	0.187(4)

At this point let us briefly summarize our findings. The critical slowing effect is substantially reduced when randomness in the exchange interactions is included in the Ising model for cluster dynamics. Nonlocal algorithms yield smaller autocorrelation times in comparison with the local algorithms due to the flip of the cluster of spins in one MCS. The presence of bond disorder results in much smaller autocorrelation times, which means that randomness facilitates obtaining different states that are statistically independent of each other through a small number of MCSs. Remarkably, the increase in autocorrelation time with lattice size is reduced with disorder strength, resulting in smaller values of the dynamic exponent.

Studies to date have shown that the addition of disorder in the Ising model leads to longer correlation times and larger critical exponent in comparison with the pure case when the

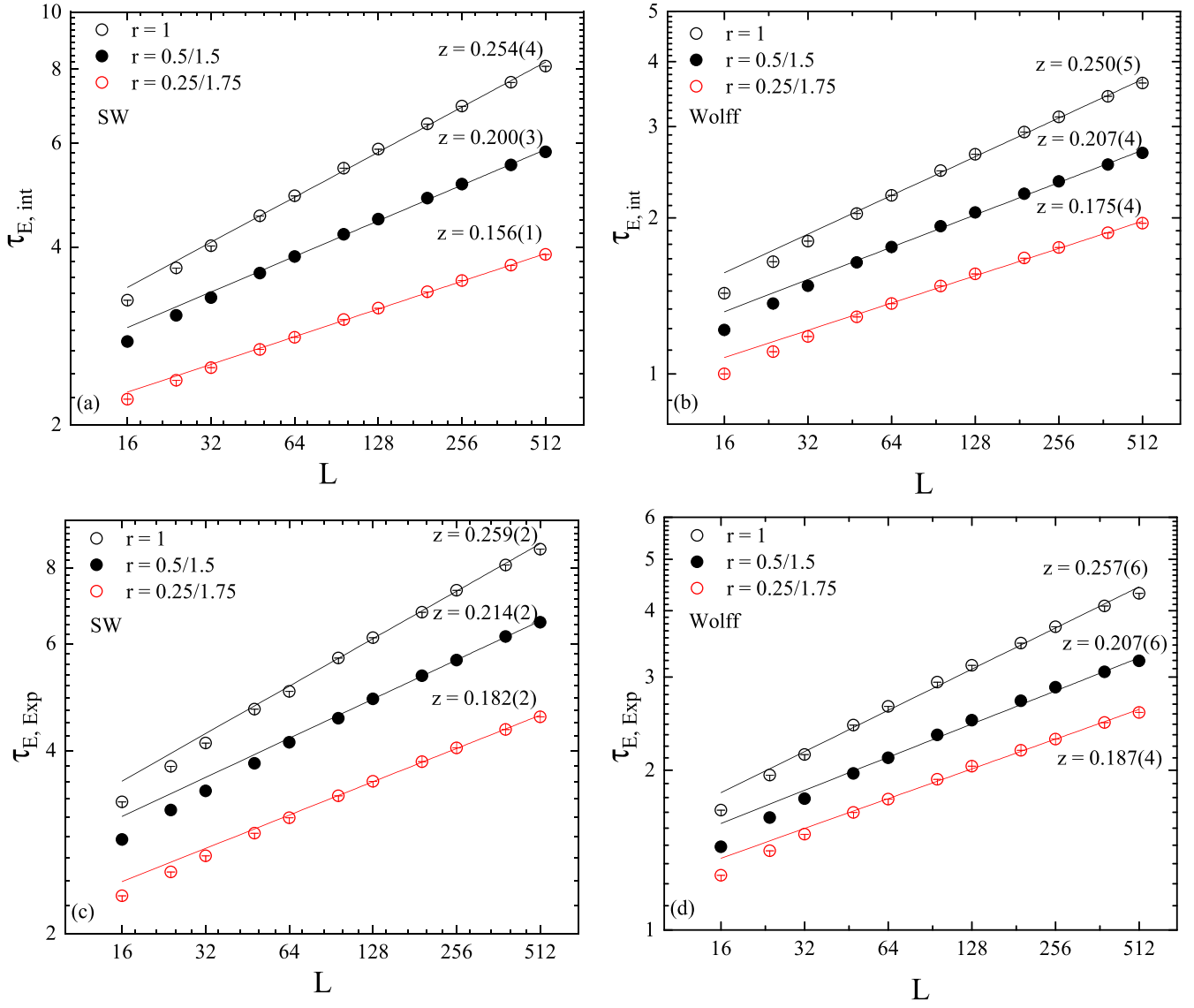

FIG. 2. Integrated and exponential autocorrelation times of energy plotted on logarithmic scales as a function of system size L for (a), (c) Swendsen-Wang and (b), (d) Wolff algorithms. The solid lines are fits of the form $\tau \sim L^z$ with the exponents given in the figure. The error bars are smaller than the symbol sizes. The smallest system size used in the fitting procedure is $L = 48$. The numerical data are obtained for three different values of the disorder parameter: $r = 1$ (upper curve), $r = 0.5/1.5$ (middle curve), and $r = 0.25/1.75$ (lower curve).

system evolves with local dynamics [21,45,52]. To observe the validity of this finding in the bond-disorder Ising model, we have performed simulations with the Metropolis algorithm for several disorder strengths at the critical temperature to determine the dynamic critical properties of the model. In the measurement of autocorrelation times, we have performed 1000 independent realizations over 1×10^6 MCSs after discarding 1×10^5 MCSs for several lattice sizes. The exponential autocorrelation times as a function of lattice size are displayed in Fig. 3. For a fixed lattice size, the autocorrelation time increases considerably when the bond disorder is included in the system. Also, if one compares the autocorrelation times of the cluster algorithms (Fig. 2) and Metropolis algorithm, it is clear that the autocorrelation times are much longer in local dynamics. For the disorder-free case, the dynamic exponent is found as $z \approx 2.15$, in agreement with the previously reported precise result [5]. Besides, the extracted critical exponents are $z \approx 2.35$ and $z \approx 2.63$ for $r = 0.5/1.5$ and $r = 0.25/1.75$, respectively. The dramatic increment in the dynamic exponents and autocorrelation times with disorder strength imply that single-spin-flip dynamics suffer from the critical slowing-down effect in the bond-disordered Ising model.

If the quenched disorder is present in a system, the measurement of an extensive thermodynamic quantity would change from sample to sample because every sample corresponds to a different disorder realization. This property of the system is called non-self-averaging. The self-averaging property of the system for any thermodynamic quantity of interest X can be tested by probing the normalized variance [53]:

$$R_X = \frac{[X^2] - [X]^2}{[X]^2}, \tag{8}$$

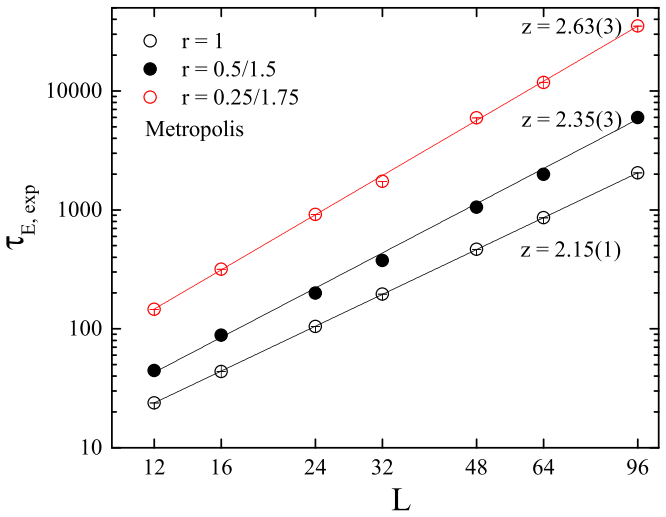

FIG. 3. Exponential autocorrelation times of energy plotted on logarithmic scales as a function of system size L for Metropolis algorithm. The solid lines are fits of the form $\tau \sim L^z$ with the exponents given in the figure. The simulations are performed for lattice sizes of $L = 12, 16, 24, 32, 48, 64, 96$. The numerical data are obtained for three different values of the disorder parameter: $r = 1$ (lower curve), $r = 0.5/1.5$ (middle curve), and $r = 0.25/1.75$ (upper curve).

where $[\cdots]$ denotes the average over different realizations. X is a self-averaging quantity if $R_X \to 0$ as $N \to \infty$. Alternatively, X is non-self-averaging if R_X goes to a constant different than zero as $N \to \infty$. This behavior of the normalized variance of a thermodynamic quantity indicates that extensive disorder averaging is required when studying disordered systems to obtain the best estimates of the observables. Self-averaging properties of disordered spin models have been previously studied by analyzing the static quantities such as energy, magnetization, specific heat, and susceptibility. In the case of the bond-disordered Ashkin-Teller model and bond-disordered four-state Potts model, the magnetization and susceptibility are found as non-self-averaging, whereas energy and specific heat are weakly self-averaging [54]. The two-dimensional site-diluted Ising model is determined to be weakly self-averaging based on the relative variance of the magnetization [55]. Non-self-averaging properties of the random-bond triangular lattice Ising model have been also demonstrated previously by observing disorder distribution of the susceptibility maxima [35].

In addition to using static quantities, non-self-averaging properties of disordered spin models can be examined by using dynamic properties such as autocorrelation times. The constant values of the square root of $R_{\tau_{E_{\text{int}}}}$ (the relative width of the probability density) for increasing system sizes suggest a broad distribution and thus demonstrate a lack of self-averaging [48]. Accordingly, we have calculated the normalized variance of autocorrelation time of energy $R_{\tau_{E_{\text{int}}}}$ from Eq. (8) by using cluster algorithms to analyze the self-averaging properties of the present model. The square root of $R_{\tau_{E_{\text{int}}}}$ as a function of the number of lattice sites N is demonstrated for the pure case ($r = 1$) and disorder strengths of $r = 0.5/1.5$ and $r = 0.25/1.75$ in Fig. 4. As one can observe, the square root of $R_{\tau_{E_{\text{int}}}}$ tends to be a constant with

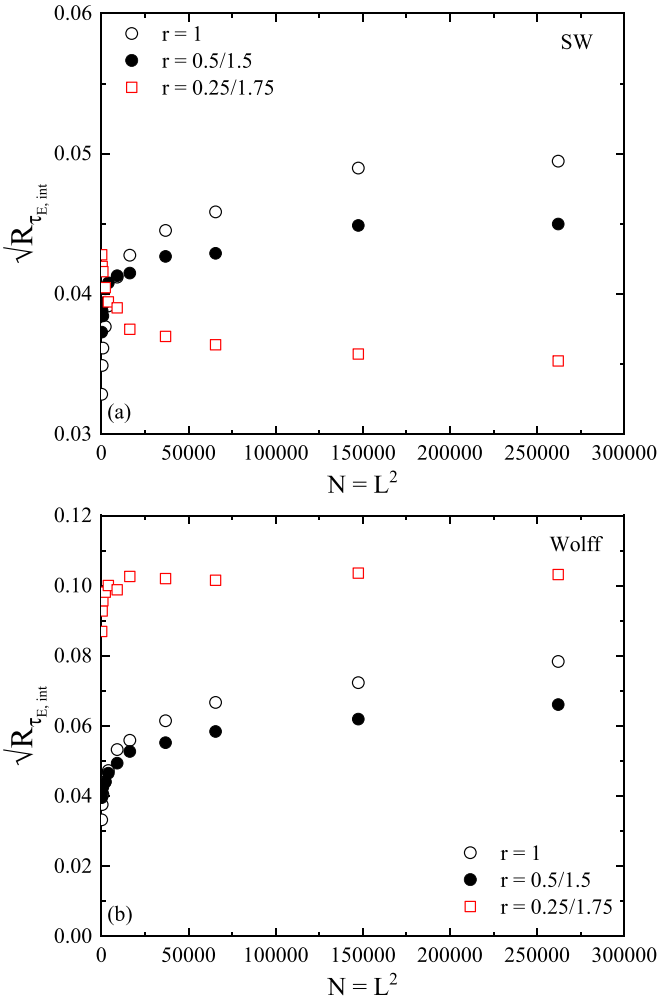

FIG. 4. Square root of $R_{\tau_{E_{\text{int}}}}$ as a function of the number of lattice sites N for the pure case ($r = 1$) and for disorder strengths of $r = 0.5/1.5$ and $r = 0.25/1.75$ obtained by using the (a) SW algorithm and (b) Wolff algorithm.

increasing system size, demonstrating the absence of self-averaging in the random-bond Ising model. Similarly, Janke and Johnston have demonstrated the lack of self-averaging in the $q = 4$ Potts model on quenched random gravity graphs by benefiting from scaled variance of autocorrelation times [48].

As a final investigation, we obtained the critical exponent ratio of magnetic susceptibility γ/ν by calculating the average cluster size $\langle C \rangle$ of the Wolff algorithm. At temperatures $T \geqslant T_C$, the mean size of the clusters flipped in the Wolff algorithm is related to the magnetic susceptibility as

$$\chi = \beta \langle C \rangle, \tag{9}$$

with $\beta = k_B T$. According to the finite-size scaling theory, the magnetic susceptibility scales with the system size as $\chi \sim L^{\gamma/\nu}$ near the critical temperature. Then it becomes possible to extract the exponent ratio γ/ν by plotting the magnetic susceptibility as defined in Eq. (9) as a function of system size at the critical temperature which is displayed in Fig. 5. The magnetic susceptibility exponent ratios are calculated as $\gamma/\nu \approx 1.75$ within the errors for the pure and disordered cases

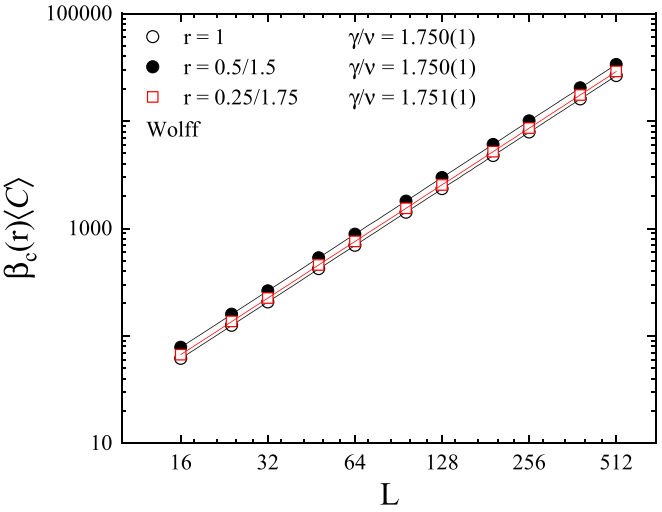

FIG. 5. Log-log plot of the magnetic susceptibility at the critical temperature as defined in Eq. (9) vs the system size for different disorder strengths. The solid lines are fits of the form $\chi \sim L^{\gamma/\nu}$. The smallest system size used in the fitting procedure is $L = 48$. The error bars are smaller than the symbol sizes.

with an excellent agreement with 2D Ising universality class. The value of the exponent ratio also supports the previous results for the 2D bond-disorder Ising model obtained using MC simulations [25,30].

IV. CONCLUSIONS

We studied the critical dynamic properties of the two-dimensional random-bond Ising model with SW and Wolff cluster algorithms. The autocorrelation times were calculated for lattice sizes up to $L = 512$ at the critical temperature. The dynamic critical exponents were estimated for several disorder strengths. Both correlation times and critical exponents were found to decrease with increasing bond randomness in the system. Based on additional simulations with the Metropolis algorithm, it was shown that the introduction of bond disorder leads to larger autocorrelation times and dynamic critical exponents. Moreover, the existence of the non-self-averaging property of the model was shown by calculating the scaled form of the standard deviation of autocorrelation times. By benefiting from the average cluster size of the Wolff algorithm, the critical exponent ratio of the magnetic susceptibility was estimated as $\gamma/\nu \approx 1.75$ within the errors, in agreement with the 2D Ising model.

The dynamic exponent of the cluster dynamics has shown a dependence on the disorder strength and therefore it can be possible to predict a functional form as $z(r)$. Our data suggested an exponential growth of the dynamic exponent with disorder parameter as $z(r) - z(1) \approx e^{-\alpha r}$, where z(1) is the dynamic exponent of the disorder-free case and α is a positive constant. In other words, as r increases (the disorder strength weakens), the dynamic exponent of the cluster algorithms increases exponentially according to our numerical data. We would also like to point out that a bimodal type of distribution ($p = 0.5$) has been considered since the critical temperature of the Ising model in the presence of the bimodal type of bond disorder is known exactly and the bimodal distribution corresponds to the strongest disorder regime. If the probabilities of the exchange-interaction strengths [Eq. (1)] were unequal, a lower disorder regime would be present and the z values would be larger than that of bimodal distribution for a fixed value of r. We should note that our test simulations performed for probabilities of $p = 0.25$ and $p = 0.75$ at $r = 0.5/1.5$ are in agreement with this expectation.

Although it is expected that the single-spin-flip algorithms suffer from the critical slowing-down effect, there are still open questions about the performance of the cluster algorithms in the disordered Ising model, q-states Potts model, and their variants. We believe that a similar situation may also be valid for disordered continuous spin models, which could be interesting to explore in the future.

ACKNOWLEDGMENTS

The numerical calculations reported in this paper were performed at TÜBİTAK ULAKBIM (Turkish agency), High Performance and Grid Computing Center (TRUBA Resources).

[1] D. P. Landau and K. Binder, *A Guide to Monte Carlo Simulations in Statistical Physics* (Cambridge University Press, Cambridge, England, 2014).
[2] M. E. J. Newman and G. T. Barkema, *Monte Carlo Methods in Statistical Physics* (Oxford University Press, New York, 1999).
[3] K. Binder and D. W. Heermann, *Monte Carlo Simulation in Statistical Physics* (Springer, Verlag, Berlin, 2010).
[4] N. Metropolis, A. W. Rosenbluth, M. N. Rosenbluth, A. H. Teller, and E. Teller, J. Chem. Phys. **21**, 1087 (1953).
[5] M. P. Nightingale and H. W. J. Blöte, Phys. Rev. Lett. **76**, 4548 (1996).
[6] R. H. Swendsen and J.-S. Wang, Phys. Rev. Lett. **58**, 86 (1987).
[7] U. Wolff, Phys. Rev. Lett. **62**, 361 (1989).
[8] U. Wolff, Phys. Lett. B **228**, 379 (1989).
[9] A. P. Young, in *Spin Glasses and Random Fields*, edited by A. P. Young (World Scientific, Singapore, 1997).
[10] A. Nihat Berker, Physica A **194**, 72 (1993).
[11] N. G. Fytas, V. Martin-Mayor, M. Picco, and N. Sourlas, J. Stat. Phys. **172**, 665 (2018).
[12] H. G. Ballesteros, L. A. Fernández, V. Martín-Mayor, A. M. Sudupe, G. Parisi, and J. J. Ruiz-Lorenzo, J. Phys. A: Math. Gen. **30**, 8379 (1997).
[13] A. B. Harris, J. Phys. C **7**, 1671 (1974).
[14] M. Fähnle, T. Holey, and J. Eckert, J. Magn. Magn. Mater. **104–107**, 195 (1992).
[15] J.-K. Kim and A. Patrascioiu, Phys. Rev. B **49**, 15764 (1994).
[16] W. Selke, L. N. Shchur, and O. A. Vasilyev, Physica A **259**, 388 (1998).
[17] P. H. L. Martins and J. A. Plascak, Phys. Rev. E **76**, 012102 (2007).

[18] M. Hasenbusch, F. P. Toldin, A. Pelissetto, and E. Vicari, Phys. Rev. E **78**, 011110 (2008).
[19] V. B. Andreichenko, W. Selke, and A. L. Talapov, J. Phys. A: Math. Gen. **25**, L283 (1992).
[20] M. Hasenbusch, F. P. Toldin, A. Pelissetto, and E. Vicari, J. Stat. Mech. (2007) P02016.
[21] W. Zhong, G. T. Barkema, and D. Panja, Phys. Rev. E **102**, 022132 (2020).
[22] A. H. Kole, G. T. Barkema, and L. Fritz, Phys. Rev. E **105**, 015313 (2022).
[23] R. Fisch, J. Stat. Phys. **18**, 111 (1978).
[24] S. Cho and M. P. A. Fisher, Phys. Rev. B **55**, 1025 (1997).
[25] J.-S. Wang, W. Selke, V. S. Dotsenko, and V. B. Andreichenko, Physica A **164**, 221 (1990).
[26] M. Hasenbusch, F. Parisen Toldin, A. Pelissetto, and E. Vicari, Phys. Rev. B **76**, 094402 (2007).
[27] N. G. Fytas and P. E. Theodorakis, Eur. Phys. J. B **86**, 30 (2013).
[28] K. Ziegler, Europhys. Lett. **14**, 415 (1991).
[29] A. L. Talapov and L. N. Shchur, J. Phys.: Condens. Matter **6**, 8295 (1994).
[30] N. G. Fytas, A. Malakis, and I. A. Hadjiagapiou, J. Stat. Mech. (2008) P11009.
[31] N. G. Fytas and A. Malakis, Phys. Rev. E **81**, 041109 (2010).
[32] I. A. Hadjiagapiou, Physica A **390**, 1279 (2011).
[33] A. Malakis, A. N. Berker, I. A. Hadjiagapiou, and N. G. Fytas, Phys. Rev. E **79**, 011125 (2009).
[34] A. Malakis, A. N. Berker, I. A. Hadjiagapiou, N. G. Fytas, and T. Papakonstantinou, Phys. Rev. E **81**, 041113 (2010).
[35] P. E. Theodorakis and N. G. Fytas, Phys. Rev. E **86**, 011140 (2012).
[36] N. G. Fytas, J. Zierenberg, P. E. Theodorakis, M. Weigel, W. Janke, and A. Malakis, Phys. Rev. E **97**, 040102(R) (2018).
[37] A. W. Sandvik, Phys. Rev. B **50**, 15803 (1994).
[38] A. W. Sandvik, Phys. Rev. B **56**, 11678 (1997).
[39] U. Kanbur, E. Vatansever, and H. Polat, Phys. Rev. B **102**, 064411 (2020).
[40] M. Acharyya, Phys. Rev. E **56**, 2407 (1997).
[41] E. Vatansever and N. G. Fytas, Phys. Rev. E **97**, 062146 (2018).
[42] E. Vatansever and N. G. Fytas, Phys. Rev. E **97**, 012122 (2018).
[43] A. Vasilopoulos, Z. D. Vatansever, E. Vatansever, and N. G. Fytas, Phys. Rev. E **104**, 024108 (2021).
[44] M. Hennecke and U. Heyken, J. Stat. Phys. **72**, 829 (1993).
[45] D. Ivaneyko, J. Ilnytskyi, B. Berche, and Yu. Holovatch, Physica A **370**, 163 (2006).
[46] W. Janke, *Monte Carlo Simulations in Statistical Physics – From Basic Principles to Advanced Applications, in Order, Disorder and Criticality* (World Scientific, Singapore, 2012), pp. 93–166.
[47] W. Janke and T. Sauer, J. Stat. Phys. **78**, 759 (1995).
[48] W. Janke and D. A. Johnston, J. Phys. A: Math. Gen. **33**, 2653 (2000).
[49] C. F. Baillie and P. D. Coddington, Phys. Rev. B **43**, 10617 (1991).
[50] P. R. A. Campos and R. N. Onody, Phys. Rev. B **56**, 14529 (1997).
[51] P. Tamayo, R. C. Brower, and W. Klein, J. Stat. Phys. **58**, 1083 (1990).
[52] H.-O. Heuer, J. Phys. A: Math. Gen. **26**, L341 (1993).
[53] S. Wiseman and E. Domany, Phys. Rev. E **58**, 2938 (1998).
[54] S. Wiseman and E. Domany, Phys. Rev. E **52**, 3469 (1995).
[55] Y. Tomita and Y. Okabe, Phys. Rev. E **64**, 036114 (2001).